2023 62nd IEEE Conference on Decision and Control (CDC)
December 13-15, 2023. Marina Bay Sands, Singapore

Neural Network Observer for Lateral Vehicle Model with Varying Sampled and Delayed Output

Hasan Abdl Ghani[1], Hind Laghmara[2], Sofiane Ahmed Ali[3], Samia Ainouz[4]

Abstract— **This research offers a neural network adaptive observer (NNAO) architecture for nonlinear lateral vehicle dynamics with variable sampled delayed output. A radial basis function (RBF) neural network is used to approximate the system's unknown part, and a new weight updating mechanism is provided. A closed-loop output predictor is used to offer inter-sample output estimate while dealing with variable samples, and a closed-loop integral compensation is used to deal with variable delay. The convergence of the proposed observer is proved using Lyapunov function and small gain arguments. Simulation tests confirm the NNAO's estimate algorithm's accuracy in estimating yaw rate, longitudinal speed, and particularly the excellent performance of the estimation of lateral speed.**

I. INTRODUCTION

Active safety vehicle systems have gained prominence due to concerns about accidents resulting from loss of vehicle control, fostering a decade-long focus on automotive research [1]. These systems enhance driving comfort and safety, incorporating features like electronic yaw stability control and anti-lock braking. Despite their wide use, challenges persist due to nonlinear system behavior, unobservable states, discrete and delayed measurements, and external disturbances. Intelligent systems research has addressed these issues, yielding diverse state observer structures.

Lateral vehicle dynamics significantly impact active safety systems, yet onboard sensors can be limited [2]. Estimating vehicle dynamics through cost-effective sensors has garnered attention, leading to two categories of techniques: kinematics-based ([3],[4]) and dynamic model-based ([5]-[7]). While kinematics-based methods suffer drift, dynamic model-based techniques demand accurate vehicle parameter knowledge. Kalman filters ([6],[9]) and robust observers ([8],[11]) attempt to mitigate these challenges, but discrepancies with real parameters and nonlinearities persist [4].

Observers often rely on known dynamics, yet real systems may contain hard-to-model parts [12]. To address this, model-free observers like neural networks ([13],[14]) have emerged. Neural networks map complex functions, with early versions designed for SISO systems [15]. Recent works extend them to MIMO systems [14], sidestepping strict SPR requirements. The authors of [14] developed a two-layer Neural Network Observer (NNO) architecture based on improved back-propagation (BP) algorithms that eliminates the SPR assumption. Chen et al. explored how uncertainty impacts lithium-ion battery system output in [16] and created a neural network adaptive observer using RBF neural network (RBFNN). Also, the NN observer was applied to vehicles, where novel estimator based on sensor fusion that includes a neural network and a linear kalman filter to estimate the vehicle roll angle was presented in [17]. In [18], the same authors created a novel observer based on H_∞ filtering in combination with a neural network (NN) for the same application.

The key problem with the preceding observers, notwithstanding their success in a variety of areas, is that they assume that the variables being measured are continuous. In real systems, this measured value, which is given by accessible sensors, is sampled. When it comes to the implementation of the mentioned observers on digital signal processors, this sensor's sampling rate may have an impact on the convergence of the proposed observers. A difficult task is determining how to create a continuous state observer based on discrete system output. There is already research on sampled data observers in the literature ([19],[20]). However, there are limited investigations on the NNO ([21],[28]). In [21], Avelar et al. suggested a differential NNO with sampling and quantization, the fundamental concept being to process sampling as a delay. Hu et al. created a deterministic learning high-gain observer under sampling conditions, however their approach is based on discrete system modeling and cannot achieve continuous state estimation [22]. In addition to the issue with sampled measurements, certain systems clearly suffer from the influence of delayed data. In the study of lateral vehicular motion, time delays have not drawn much attention. Delay, however, is a common occurrence in many processes and most natural systems. Delays, for instance, may happen as a result of information transfer between system components and insufficient information processing capabilities. Furthermore, delays must not be ignored because they may result in instability and a decrease in system performance. There have been a number of reported works that address a time-varying delay system; for comparison, see ([24],[25]). In this study, we propose a NNAO for partially unknown nonlinear systems with variable sampled delayed output. The observer's weight update rule is driven by the coordinate transformation technique reported in the literature [23], and the design of this study does not need common SPR assumptions, allowing the design to be applied in a broad range of scenarios. Inspired from [19] and [20], this paper uses a closed-loop output predictor to process the sampled output, and the Newton-Leibniz's integral method to perform integral compensation for the output of variable delay.

The rest of this paper is organized as follows: In Section

This work is co-founded by the ANR (French National Agency) through the ARTISMO project.

II, the lateral bicycle model is described and the problem statement is formulated. The proposed NNAO is given in Section III. Section IV illustrates the efficiency of the proposed method through simulation results.

II. PROBLEM STATEMENT

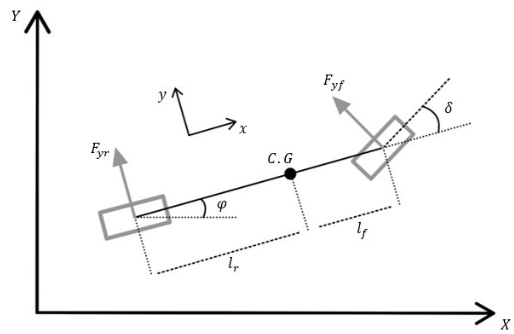

Fig. 1. 2-DOF bicycle model of the vehicle

A. DYNAMIC BICYCLE MODEL

Figure 1 depicts a two-degree-of-freedom vehicle prototype. This model is extensively used in the literature to examine lateral vehicle dynamic behavior, and it is developed by applying Newton's second law to the vehicle's longitudinal and lateral motions [1]:

$$\begin{cases} \dot{v}_x = -\frac{F_{yf}\sin\delta + F_a}{m} \\ \dot{v}_y = \frac{F_{yf}\cos\delta + F_{yr}}{m} - rv_x \\ \dot{r} = \frac{F_{yf} l_f \cos\delta - F_{yr} l_r}{I_z} \end{cases} \tag{1}$$

where in the vehicle's frame, v_x, v_y, and r represent the longitudinal, lateral, and rotational velocities respectively. The lateral forces on the front and rear tires are represented as F_{yf} and F_{yr} respectively. The force F_a is the traction force that is caused by the vehicle's motors for acceleration or brakes for deceleration, and can be calculated using the equation $F_a = ma_x$, where a_x is the inertial acceleration of the vehicle at the center of gravity in the x-axis direction. The control input, or steering angle of the front tire, is represented as δ.

Experimental evidence [26] shows that the lateral force of a tire is a non-linear function of the slip angle, and for small slip angles, it is directly proportional to the slip angle. Based on these findings, a linear tire force model and an unidentified non-linear tire force model are combined to represent the front and rear tire forces as:

$$F_{yf} = 2C_f\alpha_f + f_{yf}(\alpha_f); F_{yr} = 2C_r\alpha_r + f_{yr}(\alpha_r) \tag{2}$$

In this equation, α_f and α_r represent the slip angles of the front and rear wheels, respectively. $f_{yf}(\alpha_f)$ and $f_{yr}(\alpha_r)$ are the unknown non-linear tire force models for the front and rear wheels. For small slip angles, α_f, α_r can be approximated as:

$$\alpha_f = \delta - \frac{v_y}{v_x} - \frac{l_f r}{v_x}; \alpha_r = -\frac{v_y}{v_x} + \frac{l_r r}{v_x} \tag{3}$$

Under the assumption that the steering wheel angles are small, $\sin\delta = \delta$, equation (1) is represented in state space form, with v_x, v_y, and r being the states and the steering angle δ and the longitudinal acceleration a_x being the control inputs:

$$\begin{aligned} \dot{x} &= A(u(t), y(t))x + \varphi(u(t), x(t)) + g(u(t), x(t)) \\ y &= Cx \end{aligned} \tag{4}$$

where $x \in \mathbb{R}^3$ is the state vector, $y \in \mathbb{R}^2$ is the output matrix. $A(u, y) \in \mathbb{R}^{3\times3}$ and $\varphi(u, x) \in \mathbb{R}^3$ are nonlinear terms, and $g(u, x) \in \mathbb{R}^3$ is an unknown nonlinear term:

$$A = \begin{bmatrix} 0 & 0 & \frac{2C_f l_f \delta}{mv_x} \\ 0 & -\frac{2C_f + 2C_r}{mv_x} & 0 \\ 0 & \frac{2l_rC_r - 2l_fC_f}{Izv_x} & 0 \end{bmatrix}, C = \begin{bmatrix} 1 & 0 & 0 \\ 0 & 0 & 1 \end{bmatrix},$$

$$\varphi = \begin{bmatrix} \frac{2C_f\delta}{mv_x}v_y + a_x \\ (-v_x + \frac{2l_rC_r - 2l_fC_f}{mv_x})r + \frac{2C_f}{m}\delta \\ -\frac{2l_f^2C_f + 2l_r^2C_r}{I_zv_x}r + \frac{2C_fl_f}{I_z}\delta \end{bmatrix}, \tag{5}$$

$$g = \begin{bmatrix} \frac{1}{m}f_{yf}(\alpha_f) \\ \frac{1}{m}f_{yf}(\alpha_f) + \frac{1}{m}f_{yr}(\alpha_r) \\ \frac{l_f}{Iz}f_{yf}(\alpha_f) - \frac{l_r}{I_z}f_{yr}(\alpha_r) \end{bmatrix}.$$

B. Problem Statement and Preliminaries

In this work, we will consider that the measurements of the system are available only at sampling instant t_k, moreover, the system's inputs and output measurements also exhibit a certain amount of delay. Therefore, the system's dynamic can be described as:

$$\begin{cases} \dot{x}(t) &= A(u(t), y(t))x(t) + \varphi(u(t), x(t)) + g(u(t), x(t)) \\ y(t_k) &= Cx(t_k) \\ y_d(t) &= y(t - d(t)) \end{cases} \tag{6}$$

The sampling interval $\delta_k = t_{k+1} - t_k$ with $\delta_M = \max\{\delta_k, k \in \mathbb{N}\}$. $d(t) \in \mathbb{R}$ is the variable delayed output. Using the RBFNN's ability to approximate functions, we can estimate the nonlinear term $g(u(t), x(t))$, which is not known, in the following manner:

$$g(u, x) = \Phi(\omega)\xi + \epsilon \tag{7}$$

where $\omega = [u, x]^T$ is the input of the neural network, $\xi \in R^m$ is the weight of the neural network, $\Phi(\omega) \in R^{3\times m}$ is the matrix of the activation functions, and $\epsilon \in R^3$ is the approximation error. Each entry $\Phi_{i,j}(\omega) \in R$ in $\Phi(\omega)$ is a Gaussian function defined as follows:

$$\Phi_{i,j}(\omega) = exp(-\frac{||\omega - c_j||^2}{b_j^2}) \tag{8}$$

where $i = 1, 2, ..., n$ and $j = 1, 2, ..., m$. The centers and widths of the Gaussian functions are represented by c_i and b_i respectively. By adjusting the weight ξ appropriately, the approximation error ϵ can be kept small. This allows the RBFNN to approximate the unknown function $g(u(t), x(t))$ with a small error. It can be easily shown that the Gaussian function used as the activation function in the RBFNN is both Lipschitz and bounded. Equation (7) is frequently expressed in the literature as $W^T\Phi$ [26], with W (the weights) as a matrix and Φ as a vector. However, in the design of this work, ξ is selected to be a vector. This is due to the fact that it simplifies the design of a new adaptive weight update law, which will be addressed later.

Before discussing the main findings of this article, some technical assumptions will be presented.

Assumption 1: The state x and the input u are defined in compacts sets.

Assumption 2: The functions $A(u, x)$ and $\varphi(u, x)$ are Lipschitz with respect to x uniformly in u $\forall u \in U$, where U is a compact set.

Assumption 3: The approximation error ϵ is bounded as follows: $\epsilon \leq \epsilon_M$, where ϵ_M is a positive constant. Additionally, the weight vector ξ is restricted to a compact set, such that $\xi \leq \xi_M$, where ξ_M is a positive constant. This assumption is a common assumption in the design of neural network observers ([14]).

With the assumptions stated, we can now proceed to present the main results of the paper.

III. NEURAL NETWORK ADAPTIVE OBSERVER

A. Observer Design

The proposed observer for the class of systems defined in equation (6) has the following structure:

$$\dot{\hat{x}} = A(u, \hat{y})\hat{x} + \varphi(u, \hat{x}) + \Phi(u, \hat{x})\hat{\xi} - (L + \chi P \Xi^T)(C\hat{x} - w) \tag{9}$$

$$\begin{cases} \dot{w_d}(t) &= C\bigg(A(u(\delta_t), \hat{y}(\delta_t))\hat{x}(\delta_t) + \varphi(u(\delta_t), \hat{x}(\delta_t)) + \\ & \quad \Phi(u(\delta_t), \hat{x}(\delta_t))\hat{\xi}(\delta_t)\bigg) - K_1(C\hat{x}(\delta_t) - w_d(t)) \\ & \quad \text{for } \ t \in [t_k, t_{k+1}) \\ w(t_k - d(t)) = y(t_k - d(t)) \end{cases} \tag{10}$$

with

$$w = w_d + \int_{\delta_t}^{t} \bigg[C\bigg(A(u(s), \hat{y}(s))\hat{x}(s) + \varphi(u(s), \hat{x}(s)) + \Phi(u(s), \hat{x}(s), \hat{\xi}(s))\bigg) - K_2(C\hat{x}(s) - w(s))\bigg] ds \tag{11}$$

where $\hat{x} \in R^3$ is the estimated state, $w \in R^2$ is the predicted output, $\hat{\xi} \in R^m$ is the estimated weight. $\hat{y} = C\hat{x}$ and $\delta_t = t - d(t)$. P $\in R^{m\times m}$ is a symmetric positive definite (SPD) matrix . L $\in R^{3\times 2}$ is the observer gain that will be designed to ensure $A(u, \hat{y}) - LC$ is Hurwitz. $K_1 \in R^{2\times 2}$ and $K_2 \in R^{2\times 2}$ are predictor gains. $\Xi = C\chi$, where $\chi \in R^{3\times m}$ is an auxiliary variable that fulfills:

$$\dot{\chi} = (A(u, y) \hat{-} LC)\chi + \Phi(u, \hat{x}) \tag{12}$$

Clearly, the observer structure is made up of three parts. Equation (9) is an observer for state estimation of system (6). Equation (10) is the output predictor, which provide a piecewise continuous estimation of y(t). $K_1(C\hat{x}(\delta_t) - w_d(t))$ is a corrective term used to improve the output predictor's performance. Equation (11) allows the observer to compensate for the delay affecting the system output.

Remark 1: Because $A(u, \hat{y}) - LC$ is Hurwitz and Φ is bounded, it is easy to derive that χ is bounded as well.

Remark 2: The weighting update law (13) does not require the persistent excitation assumption due to the Gaussian function's constant positive character.

B. Stability Analysis

The stability of the proposed observer (9-11) is given by the following Theorem.

Theorem 1: Under Assumption 1-3, system (9-11) is a NNAO for system (6), with the following neural network adaptive weight update law:

$$\dot{\hat{\xi}} = -P\Xi^T(C\hat{x} - w) - \theta\hat{\xi} \tag{13}$$

where θ is a positive constant that needs to be designed. If the maximum of the sampling interval δ_M and the maximum delay d_M satisfy the following conditions:

$$\begin{cases} 0 < ||K_1||\delta_M e^{\alpha\delta_M} < 1 \\ 0 < ||K_2||d_M e^{\alpha d_M} < 1 \\ 0 < r_1(d, \delta_M) < 1 \end{cases}$$

with

$$\alpha_0 = \theta_m - k - \frac{c}{2}, \theta_m = min\bigg(\frac{\lambda_m(Q)}{\lambda_M(S)}, 2\theta\bigg),$$

$\ni$ constant α such that $0 < \alpha < \alpha_0/2$,

$$r_1(d, \delta_M) = \frac{2c_5 w_1 d_M e^{\alpha d_M}}{\alpha_0(1 - ||K_2||d_M e^{\alpha d_M})} + \frac{2c_5 w_1 \delta_M e^{\alpha\delta_M}}{\alpha_0(1 - ||K_1||\delta_M e^{\alpha\delta_M})(1 - ||K_2||d_M e^{\alpha d_M})},$$

$$k = k_0 + k_1 + k_2, c = c_0 + c_1 + c_2 + c_3,$$

$$k_0 = 2\alpha_\gamma L_A x_M||C||, c_0 = 2\alpha_\beta L_A x_M||C||\chi_M,$$

$$k_1 = 2\alpha_\gamma L_\Phi \xi_M, c_1 = 2\alpha_\beta L_\Phi \xi_M \chi_M,$$

$$k_2 = 2\alpha_\beta L_\Phi \chi_M, c_3 = 2\alpha_\beta \Phi_M, \alpha_\gamma = \sqrt{\lambda_M(S)/\lambda_m(S)}$$

$$c_5 = max\bigg(2||L||\sqrt{\lambda_m(S)}, \frac{2\Xi_M}{\sqrt{\lambda_M(P)}}\bigg),$$

$$w_1 = max\bigg(\frac{\Theta + L_A||C||^2 x_M + ||C||L_\phi + ||C||L_\Phi\xi_M}{\sqrt{\lambda_m(S)}}, \frac{(\Theta + L_A||C||^2 x_M + ||C||L_\phi + ||C||L_\Phi\xi_M)\chi_M}{\sqrt{\lambda_M(P)}}\bigg),$$

$$\Theta = \sup_{t\geq 0}||CA(u, \hat{y}) - KC||, \chi_M = \sup_{t\geq 0}||\chi||, \Xi = \sup_{t\geq 0}||\Xi||,$$

$$\alpha_\beta = \sqrt{\lambda_M(S)/\lambda_M(P)}$$

then the state and weight estimation are uniformly ultimately bounded (UUB).

Proof: Define the system state error $\tilde{x} = \hat{x} - x$ and weight error $\tilde{\xi} = \hat{\xi} - \xi$, then:

$$\begin{cases} \dot{\tilde{x}} &= A_c\tilde{x} + \tilde{A}(u,y,\hat{y})x + \tilde{\varphi}(u,\hat{x},x) + \tilde{\Phi}(u,\hat{x},x)\xi + \\ & \quad \Phi(u,\hat{x})\tilde{\xi} - \epsilon + \chi\dot{\tilde{\xi}} + \theta\chi\tilde{\xi} + \theta\chi\xi + Le_w \\ \dot{\tilde{\xi}} &= -P\Xi^T C\tilde{x} - \theta\tilde{\xi} + \theta\xi + P\Xi^T e_w \end{cases} \tag{14}$$

where $A_c = A(u,\hat{y}) - LC$, $\tilde{A}(u,y,\hat{y}) = A(u,\hat{y}) - A(u,y)$, $\tilde{\Phi}(u,\hat{x},x) = \Phi(u,\hat{x}) - \Phi(u,x)$ and $\tilde{\varphi}(u,\hat{x},x) = \varphi(u,\hat{x}) - \varphi(u,x)$.

Let's now introduce the coordinate transformation suggested in [23]:

$$\zeta(t) = \tilde{x}(t) - \chi\tilde{\xi}(t) \tag{15}$$

Differentiating $\zeta(t)$ with respect to time:

$$\begin{aligned} \dot{\zeta}(t) &= A_c\zeta + \tilde{A}(u,y,\hat{y})x + \tilde{\varphi}(u,\hat{x},x) - \epsilon + \tilde{\Phi}(u,\hat{x},x)\xi \\ &\quad + \theta\chi\tilde{\xi} + \theta\chi\xi + Le_w \end{aligned} \tag{16}$$

Taking into account the following Lyapunov function:

$$V(\zeta,\tilde{\xi}) = V_1(\zeta) + V_2(\tilde{\xi}) \tag{17}$$

with

$$V_1(\zeta) = \zeta^T S\zeta \tag{18}$$

$$V_2(\tilde{\xi}) = \tilde{\xi}^T P^{-1}\tilde{\xi} \tag{19}$$

where S satisfies $Ac^T + SA_c \leq -Q - C^TC$.

Then differentiating $V_1(\zeta)$ with respect to time , one gets:

$$\begin{aligned} \dot{V}_1(\zeta) &= 2\zeta^T SA_c\zeta + 2\zeta^T S\tilde{A}(u,y,\hat{y})x + 2\zeta^T S\tilde{\varphi}(u,\hat{x},x) \\ &\quad + 2\zeta^T S\tilde{\Phi}(u,\hat{x},x)\xi - 2\zeta^T S\epsilon + 2\theta\zeta^T S\chi\tilde{\xi} \\ &\quad + 2\theta\zeta^T S\chi\xi + 2\zeta^T SLe_w \end{aligned} \tag{20}$$

According to (16), we get:

$$||\tilde{x}|| \leq ||\zeta|| + ||\chi||||\tilde{\xi}|| \leq ||\zeta|| + \chi_M||\tilde{\xi}|| \tag{21}$$

Taking the nonlinear terms of (20), we have:

$$\begin{aligned} 2\zeta^T S\tilde{A}(u,y,\hat{y})x &\leq 2\sqrt{\lambda_M(S)}\sqrt{V_1(\zeta)}L_A x_M||C||||\tilde{x}|| \\ &\leq k_0V_1 + c_0\sqrt{V_1}\sqrt{V_2} \\ 2\zeta^T S\tilde{\Phi}(u,x,\hat{x})\xi &\leq 2\sqrt{\lambda_M(S)}\sqrt{V_1(\zeta)}L_\Phi\xi_M||\tilde{x}|| \\ &\leq k_1V_1 + c_1\sqrt{V_1}\sqrt{V_2} \\ 2\zeta^T S\tilde{\varphi}(u,x,\hat{x}) &\leq 2\sqrt{\lambda_M(S)}\sqrt{V_1(\zeta)}L_\varphi||\tilde{x}|| \\ &\leq k_2V_1 + c_2\sqrt{V_1}\sqrt{V_2} \\ 2\theta\zeta^T S\chi\tilde{\xi} &\leq 2\sqrt{\lambda_M(S)}\sqrt{V_1(\zeta)}\chi_M||\tilde{\xi}|| \\ &\leq +c_3\sqrt{V_1}\sqrt{V_2} \end{aligned} \tag{22}$$

By combing (20) and (22), we have:

$$\begin{aligned} \dot{V}_1(\tilde{\zeta}) &\leq -\zeta^T Q\zeta - \zeta^T C^T C\zeta + kV_1 + c\sqrt{V_1}\sqrt{V_2} \\ &\quad + 2\sqrt{\lambda_M(S)V_1}\epsilon_M + 2\sqrt{\lambda_M(S)V_1}\chi_M\xi_M \\ &\quad + 2||L||\sqrt{\lambda_M(S)V_1}||e_w|| \end{aligned} \tag{23}$$

By taking $V_2(\zeta)$ and differentiating is w.r.t. time, one gets:

$$\begin{aligned} \dot{V}_2(\tilde{\xi}) &= -2\theta V_2 - \tilde{\xi}^T\Xi^T\Xi\tilde{\xi} - 2\tilde{\xi}^T\Xi^T C\zeta + 2\tilde{\xi}^T\Xi^T e_w \\ &\leq -2\theta V_2 - \tilde{\xi}^T\Xi^T\Xi\tilde{\xi} - 2\tilde{\xi}^T\Xi^T C\zeta \\ &\quad + 2\Xi_M\sqrt{\frac{V_2}{\lambda_M(P)}}||e_w|| \end{aligned} \tag{24}$$

By introducing a change of coordinates $W = \sqrt{V_1} + \sqrt{V_2}$, following (23-24), we have:

$$\dot{W} = -\alpha_0 W + c_5||e_w|| + c_4 \tag{25}$$

Integrating and then multiplying both sides of (25) by $e^{\alpha t}$, knowing that $e^{-(\alpha_0-\alpha)} \leq 1$, we have:

$$\begin{aligned} e^{\alpha t}W &\leq w_0 + e^{(-\alpha_0-\alpha)t}c_4\int_{t_k}^t e^{(\alpha_0-\alpha)t}e^{\alpha_0 s}ds \\ &\quad + e^{(-\alpha_0-\alpha)t}c_5\int_{t_k}^t e^{(\alpha_0-\alpha)t}e^{\alpha_0 s}||e_w||ds \\ &\leq w_0 + e^{(-\alpha_0-\alpha)t}c_4\int_{t_k}^t e^{(\alpha_0-\alpha)t}ds \sup_{t_0\leq s\leq t}(e^{\alpha s}) \\ &\quad + e^{(-\alpha_0-\alpha)t}c_5\int_{t_k}^t e^{(\alpha_0-\alpha)t}ds(e^{\alpha_0 s}\sup_{t_0\leq s\leq t}(e^{\alpha s}||e_w||) \end{aligned} \tag{26}$$

where $w_0 = e^{\alpha_0 t_0}W(t_0)$. Taking $0 < \alpha < \alpha_0/2$, then:

$$e^{\alpha t}W \leq w_0 + \frac{2c_4}{\alpha_0}e^{\alpha t} + \frac{2c_5}{\alpha_0}\sup_{t_0\leq s\leq t}(e^{\alpha s}||e_w||) \tag{27}$$

On the other hand, lets define the system' output error as $e_w = w - y$, then we have:

$$\begin{aligned} ||e_w|| &= ||w-y|| \leq e_{wd} + w_1\int_{t-d_M}^t e^{-\alpha s}e^{\alpha s}W(s)ds \\ &+ ||K_2||\int_{t-d_M}^t e^{-\alpha s}e^{\alpha s}||e_w(s)||ds + v_1\int_{t-d_M}^t e^{-\alpha s}e^{\alpha s}ds \\ ||e_w|| &\leq e_{wd} + w_1\int_{t-d_M}^t e^{-\alpha s}\sup_{t-d_M\leq s\leq t}(e^{\alpha s}W(s))ds \\ &\quad + ||K_2||\int_{t-d_M}^t e^{-\alpha s}\sup_{t-d_M\leq s\leq t}(e^{\alpha s}||e_w(s)||)ds \\ &\quad + v_1\int_{t-d_M}^t e^{-\alpha s}\sup_{t-d_M\leq s\leq t}(e^{\alpha s})ds \end{aligned} \tag{28}$$

Using the mean-value theorem, $\exists\, \rho \in [t-d_M, t]$, then:

$$\int_{t-d_M}^t e^{-\alpha s}ds \leq d_M e^{-\rho\alpha} \leq d_M e^{-\alpha t_k} \tag{29}$$

Combining (29) and (30), and multiplying both sides by $e^{\alpha t}$, we get:

$$\begin{aligned} &\sup_{t_0\leq s\leq t}(||e_w||e^{\alpha t}) \leq \sup_{t_0\leq s\leq t}(||e_{wd}||e^{\alpha t}) \\ &\quad + w_1 d_M e^{\alpha d_M}\sup_{t_0\leq s\leq t}(e^{\alpha s}W) + v_1 d_M e^{\alpha d_M}\sup_{t_0\leq s\leq t}(e^{\alpha s}) \\ &\quad + ||K_2||d_M e^{\alpha d_M}\sup_{t_0\leq s\leq t}(e^{\alpha s}||e_w(s)||) \end{aligned} \tag{30}$$

If d_M satisfy $0 < ||K_2||d_M e^{\alpha d_M} < 1$, then:

$$\begin{aligned}\sup_{t_0\le s\le t}(e^{\alpha s}||e_w||) \le \Bigg(&\sup_{t_0\le s\le t}(e^{\alpha s}||e_{wd}||) + v_1 d_M e^{\alpha d_M} e^{\alpha t} \\ &+ w_1 d_M e^{\alpha d_M}\sup_{t_0\le s\le t}(e^{\alpha s}W)\Bigg)/(1-||K_2||d_M e^{\alpha d_M})\end{aligned} \tag{31}$$

Similar as (29-30), if δ_M satisfy $0 < ||K_1||\delta_M e^{\alpha\delta_M} < 1$, then:

$$\begin{aligned}\sup_{t_0\le s\le t}(e^{\alpha s}||e_{wd}||) \le & (w_1\delta_M e^{\alpha\delta_M}\sup(e^{\alpha(s-d(t))}W(s-d(t))) \\ &+ v_1\delta_M e^{\alpha d_M}e^{\alpha t})/(1-||K_1||\delta_M e^{\alpha\delta_M})\end{aligned} \tag{32}$$

Combing the last two equations, we get:

$$\begin{aligned}&\sup_{t_0\le s\le t}(e^{\alpha s}||e_w||) \le \\ &\frac{w_1 d_M e^{\alpha d_M}\sup_{t_0\le s\le t}(e^{\alpha s}W) + v_1 d_M e^{\alpha d_M}e^{\alpha t}}{1-||K_2||d_M e^{\alpha d_M}} + \\ &\frac{w_1\delta_M e^{\alpha\delta_M}\sup_{t_0\le s\le t}(e^{\alpha(s-d(t))}W(s-d(t))) + v_1\delta_M e^{\alpha\delta_M}e^{\alpha t}}{(1-||K_1||\delta_M e^{\alpha\delta_M})(1-||K_2||d_M e^{\alpha d_M})}\end{aligned} \tag{33}$$

Taking (30) and (27), then:

$$\begin{aligned}e^{\alpha t}W(t) &\le w_0 + \frac{2c_4}{\alpha_0}e^{\alpha t} + \frac{2c_5}{\alpha_0}\sup_{t_0\le s\le t}(e^{\alpha s}||e_w||) \\ &\le w_2 + r_1(d,\delta_M)\sup_{t_0\le s\le t}(e^{\alpha s}W) + r_2(d,\delta_M,\epsilon)e^{\alpha t}\end{aligned} \tag{34}$$

with

$$\begin{aligned}w_2 &= w_0 + \frac{2c_5 w_1\delta_M e^{\alpha\delta_M}\sup_{-d_M\le s\le t_0}(e^{\alpha(s)}W(s))}{\alpha_0(1-||K_1||\delta_M e^{\alpha\delta_M})(1-||K_2||d_M e^{\alpha d_M})} \\ r_1(d,\delta_M) &= \frac{2c_5 w_1 d_M e^{\alpha d_M}}{\alpha_0(1-||K_2||d_M e^{\alpha d_M})} \\ &\quad + \frac{2c_5 w_1\delta_M e^{\alpha\delta_M}}{\alpha_0(1-||K_1||\delta_M e^{\alpha\delta_M})(1-||K_2||d_M e^{\alpha d_M})} \\ r_2(d,\delta_M,\epsilon) &= \frac{2c_5 v_1 d_M e^{\alpha d_M}}{\alpha_0(1-||K_2||d_M e^{\alpha d_M})} \\ &\quad + \frac{2c_5 v_1\delta_M e^{\alpha\delta_M}}{\alpha_0(1-||K_1||\delta_M e^{\alpha\delta_M})(1-||K_2||d_M e^{\alpha d_M})}\end{aligned} \tag{35}$$

Let d_M and δ_M satisfy:

$$r_1(d,\delta_M) < 1 \tag{36}$$

we will have:

$$W(t) \le \frac{w_2 e^{-\alpha t} + r_2(d,\delta_M,\epsilon)}{1-r_1(d,\delta_M} \tag{37}$$

(37) indicates that ζ and ξ exhibit UUB characteristics. It can be deduced from (15), then, that $\tilde{x}$ exhibits the properties of UUB. End of proof ■

IV. Simulation Results

In this section, we gathered relevant data and performed simulations for validation. The data collection involved using the experimental Citroen AMI at the IRSEEM facility in Rouen, France. We subsequently performed simulations and comparisons, demonstrating the effectiveness of our proposed observer. The car's parameters are shown in Table 1.

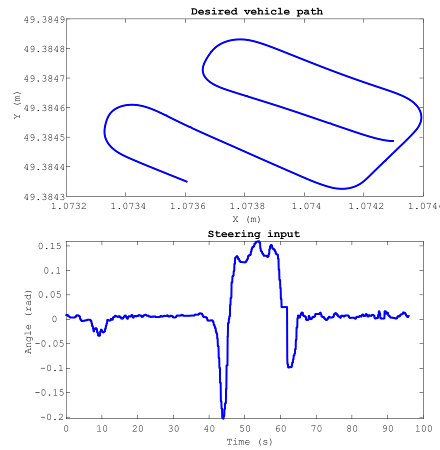

Fig. 2. RTMaps simulation results: desired vehicle path, and steering input.

TABLE I
PARAMETER VALUES OF VEHICLE MODEL

Parameter	Description	Value
m	Vehicle Mass	600 [kg]
I_z	Vehicle yaw moment of inertia	1100 $[kgm^2]$
l_f	Distance from CoG to front axle	0.86 [m]
l_r	Distance from CoG to rear axle	0.9 [m]
C_f	Front cornering stiffness	27500 [N/rad]
C_r	Rear cornering stiffness	27500 [N/rad]

For the simulation, the vehicle was maneuvered via the parking lot, as shown in Fig. 2, and the steering input required to keep the planned vehicle route is also depicted. Fig. 3 show the considered variable delay in the simulation. A random sample time is selected, ranging from $T_s = 0.05$ to $T_s = 0.3$. 15 neurons were selected in the hidden layer. In the simulation, the following parameters are chosen: $\chi(0) = 0_{3\times 15}, K_1 = 30I_2, K_2 = 20I_2, P = 20diag(0.1I_{15}, 7I_{15}, I_{15}), \theta = 0.4, L = [50\ 10; 15\ -5; -30\ 20]$. As depicted in Fig 4, in the context of estimating the system states with variable sampled delayed output, a comparative analysis between Observer 1 (proposed observer) and Observer 2 (same observer without delay compensation) was conducted to assess the impact of delay on the system. Remarkably, Observer 1 exhibited significantly superior performance in accurately estimating the vehicle state.

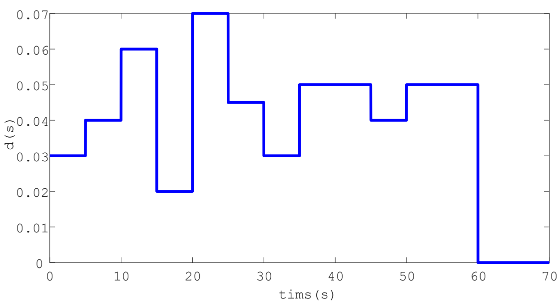

Fig. 3. Evolution of the random delay d(t)

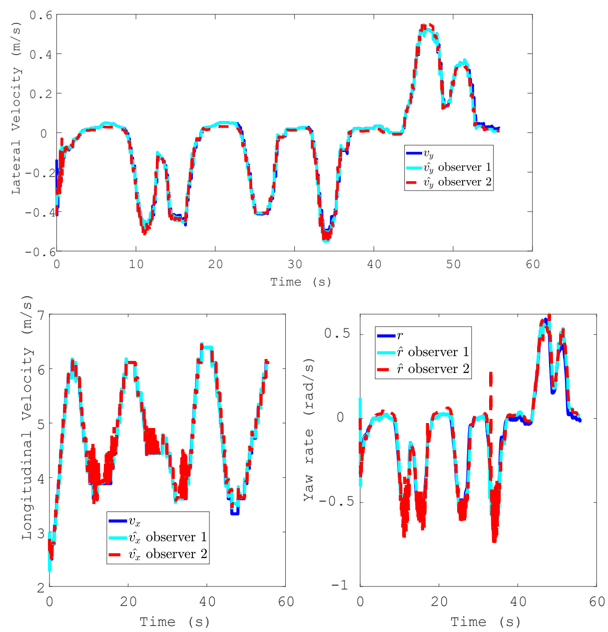

Fig. 4. RTMaps simulation results : estimation of vehicle state variables.

REFERENCES

[1] R. Rajamani, Vehicle Dynamics and Control. Springer US, 2012.

[2] D. Piyabongkarn, R. Rajamani, J. A. Grogg and J. Y. Lew, "Development and experimental evaluation of a slip angle estimator for vehicle stability control," American Control Conference, pp. 6, 2006.

[3] G. H. Fjær, L. S. Imsland, T.-A Johansen, J, C. Kalkkuhl and A. Suissa. "Vehicle Sideslip Estimation Design , implementation , and experimental validation," 2009.

[4] D. Selmanaj, M. Corno, G. Panzani and S.-M. Savaresi, "Vehicle sideslip estimation: A kinematic based approach," Control Engineering Practice, vol. 67, pp. 1-12, 2017.

[5] K. Nam, S. Oh, H. Fujimoto and Y. Hori, "Vehicle state estimation for advanced vehicle motion control using novel lateral tire force sensors," Proceedings of the 2011 American Control Conference, pp. 4853-4858, 2011.

[6] T. Zhu and H. Zheng, "Application of Unscented Kalman Filter to Vehicle State Estimation," ISECS International Colloquium on Computing, Communication, Control, and Management, pp. 135-139, 2008.

[7] A.-T. Nguyen, T.-M. Guerra, C. Sentouh and H. Zhang, "Unknown Input Observers for Simultaneous Estimation of Vehicle Dynamics and Driver Torque: Theoretical Design and Hardware Experiments," IEEE/ASME Transactions on Mechatronics, vol. 24, no. 6, pp. 2508-2518, Dec. 2019.

[8] A.-T. Nguyen, T. Q. Dinh, T.-M. Guerra and J. Pan, "Takagi–Sugeno Fuzzy Unknown Input Observers to Estimate Nonlinear Dynamics of Autonomous Ground Vehicles: Theory and Real-Time Verification," IEEE/ASME Transactions on Mechatronics, Institute of Electrical and Electronics Engineers, vol. 26, pp.1328-1338, 2021.

[9] M. Doumiati, A. C. Victorino, A. Charara and D. Lechner, "Onboard Real-Time Estimation of Vehicle Lateral Tire–Road Forces and Sideslip Angle," IEEE/ASME Transactions on Mechatronics, vol. 16, no. 4, pp. 601-614, Aug. 2011.

[10] H. Du, J. Lam, K. C. Cheung, W. Li and N. Zhang, "Side-slip angle estimation and stability control for a vehicle with a non-linear tyre model and a varying speed," Proceedings of the Institution of Mechanical Engineers, Part D: Journal of Automobile Engineering, vol. 229, pp. 486-505, 2015.

[11] D. Meizel, J. Stephant and A. Charara, "Evaluation of a sliding mode observer for vehicle sideslip angle," Control Engineering Practice, Elsevier, vol. 15, pp. 803-812, 2007.

[12] A. N. Lakhal, A. S. Tlili, N. B. Braiek, "Neural Network Observer for Nonlinear Systems Application to Induction Motors 1," International Journal of Control and Automation, 2010.

[13] R. Rahimilarki, Z. Gao, A. Zhang and R. Binns, "Robust Neural Network Fault Estimation Approach for Nonlinear Dynamic Systems With Applications to Wind Turbine Systems," IEEE Transactions on Industrial Informatics, vol. 15, no. 12, pp. 6302-6312, Dec. 2019.

[14] F. Abdollahi, H. A. Talebi and R. V. Patel, "A stable neural network-based observer with application to flexible-joint manipulators," IEEE Transactions on Neural Networks, vol. 17, no. 1, pp. 118-129, Jan. 2006.

[15] D. Strobl, U. Lenz and D. Schroder, "Systematic design of stable neural observers for a class of nonlinear systems," Proceedings of the 1997 IEEE International Conference on Control Applications, Hartford, CT, USA, pp. 377-382, 1997.

[16] N. Chen, X. Zhao, J. Chen, X. Xu, P. Zhang, W. Gui," Design of a Non-Linear Observer for SOC of Lithium-Ion Battery Based on Neural Network," Energies 2022, 15, 3835.

[17] L. V. Meléndez, , B. L. Boada, M.-J. L. Boada, AA. Gauchía and V. Díaz, "A Sensor Fusion Method Based on an Integrated Neural Network and Kalman Filter for Vehicle Roll Angle Estimation," vol. 16, no. 9, 2016.

[18] B. L. Boada, M.-J. L. Boada, L. V. Melendez and V. Diaz, "A robust observer based on H∞ filtering with parameter uncertainties combined with Neural Networks for estimation of vehicle roll angle," Mechanical Systems and Signal Processing, vol. 99, pp. 611-623, 2018.

[19] I. Karafyllis and C. Kravaris, "From Continuous-Time Design to Sampled-Data Design of Observers," in IEEE Transactions on Automatic Control, vol. 54, no. 9, pp. 2169-2174, Sept. 2009.

[20] C. Song, H. Wang, Y. Tian and G. Zheng, "Event-Triggered Observer Design for Delayed Output-Sampled Systems," in IEEE Transactions on Automatic Control, vol. 65, no. 11, pp. 4824-4831, Nov. 2020.

[21] A. Avelar, I. Salgado, H. Ahmed, M. Mera, I. Chairez, "Differential neural networks observer for second order systems with sampled and quantized output," IFAC-PapersOnLine, vol. 51, pp. 490-495, 2018.

[22] J. Hu, W. Wu, B. Ji and C. Wang, "Observer Design for Sampled-Data Systems via Deterministic Learning," in IEEE Transactions on Neural Networks and Learning Systems, vol. 33, no. 7, pp. 2931-2939, July 2022.

[23] Q. Zhang, "Adaptive observer for multiple-input-multiple-output (MIMO) linear time-varying systems," in IEEE Transactions on Automatic Control, vol. 47, no. 3, pp. 525-529, March 2002.

[24] H. E. Aiss, K. A. Barbosa and A. A. Peters, "Nonlinear Time-Delay Observer-Based Control to Estimate Vehicle States: Lateral Vehicle Model," in IEEE Access, vol. 10, pp. 110459-110472, 2022.

[25] A. Seuret, F. Gouaisbaut, "Wirtinger-based integral inequality: Application to time-delay systems," in Automatica, vol. 49, pp. 2860-2866, 2013.

[26] H. Pacejka, Tire and vehicle dynamics. Elsevier 2005.

[27] X. Liu, C. Yang, Z. Chen, M. Wang, C.Y. Su, "Neuro-adaptive observer based control of flexible joint robot," Neurocomputing, vol. 275, pp. 73-82, 2018.

[28] A.-G. Hasan, H. Laghmara, A.-A. Sofiane, S. Ainouz, G. Xing, "Continuous–Discrete Time Neural Network Observer for Nonlinear Dynamic Systems Application to Vehicle Systems," in 22nd World Congress of the International Federation of Automatic Control, Jul 2023.